Available online at www.sciencedirect.com
SCIENCE DIRECT®
Journal of Organometallic Chemistry 690 (2005) 1332–1339
Journal of Organometallic Chemistry
www.elsevier.com/locate/jorganchem

Synthesis and X-ray structure study on new Au(I) polymer architectures based on multi-sulfur tentacles

Keiko Nunokawa [a], Kazuya Okazaki [a], Satoru Onaka [a,*], Mitsuhiro Ito [a], Tetsuya Sunahara [a], Tomoji Ozeki [b], Hiroyuki Imai [c], Katsuya Inoue [c]

[a] *Department of Environmental Technology, Graduate School of Engineering, Nagoya Institute of Technology, Gokiso-cho, Showa-ku, Nagoya 466-8555, Japan*
[b] *Department of Chemistry and Materials Science, Tokyo Institute of Technology, O-okayama, Meguro-ku, Tokyo 152-8551, Japan*
[c] *Institute for Molecular Science, Myodaiji, Okazaki 444-8585, Japan*

Received 13 August 2004; accepted 4 October 2004
Available online 7 February 2005

Abstract

Multi-thiolate ligands are used as a scaffold to construct a series of supramolecules, which cover the following entries; $[(1,3\text{-}S_2\text{–}C_6H_4)\{AuP(C_6H_4\text{–}3\text{-}CF_3)_3\}_2]_n$ (**1**), $[(1,4\text{-}S_2\text{–}C_6H_4)\{AuP(C_6H_4\text{–}3\text{-}CF_3)_3\}_2]_n$ (**2**), $(1,4\text{-}S_2\text{–}C_6H_4)\{AuP(C_6H_5)_2(2\text{-pyridine})\}_2$ (**3**), $[(1,3,5\text{-}S_3\text{–}C_6H_3)\{AuP(C_6H_5)_2(2\text{-pyridine})\}_3]_n$ (**4**), and $[(1,3,5\text{-}S_3\text{–}C_6H_3)\{AuP(C_6H_4\text{–}3\text{-}CF_3)_3\}_3]_n$ (**5**). The molecular and crystal structures of these new derivatives have been elucidated by single crystal X-ray diffraction. Aurophilic interactions have been demonstrated for **1**, **2**, **4**, and **5** to produce new supramolecular architectures. Nano-channels are formed by aurophilic and π–π interactions for **1**, in which benzene molecules are trapped. An 8 (eight)-shaped loop is formed in solid state for **2**. Infinite zigzag chains are constructed for **4** and **5**.

Keywords: Aurophilicity; Multi-S ligands; Supramolecules; Dendrimers; Helical structures

1. Introduction

The design and the synthesis of supramolecular structures in the solid state have attracted keen interest not only because of topological beauty [1] but also of recent applications to nano-technologies [2]. The use of aurophilic interaction has led to many fruitful outcomes for constructing gold-based extended structures, which should serve as such prospective nano-materials [3]. Thiolate ligands are especially attractive scaffold to build-up such nano-molecules [4–7]. In this vein, trithiocyanuric acid, its salts, and its derivatives are intriguing and many fantastic supramolecules have been reported recently [8–11]. Schmidbaur and co-workers [12] have synthesized interesting supramolecules by the use of 1,3,4-thiadiazole-2,5-dithiolate, which is similar to the above ligands. We have also been interested in using thiolate ligands to control aurophilicity [4] and led to explore a pre-dendrimer chemistry based on multi-sulfur tentacles as a logical extension of our research programs. 1,3- and 1,4-Dimercaptobenzene and 1,3,5-trimercaptobenzene are our choice in addition to the above trithiocyanurates, on which a unique Au_{12} cluster has been constructed recently [4d]. In the present study, these multi-thiolate ligands were reacted with two kinds of gold phosphine chlorides where the phosphine represents $P(C_6H_4\text{–}3\text{-}CF_3)_3$ and $P(C_6H_5)_2$(2-pyridine) other than PPh_3. These ligands were chosen because of the following two reasons: the selection of $P(C_6H_4\text{–}3\text{-}CF_3)_3$ was rationalized in the previous paper in order to reinforce the aurophilicity [4b]. $P(C_6H_5)_2$(2-pyridine) was expected to exhibit

* Corresponding author. Tel.: +81527355160; fax: +81527355160.
E-mail address: onaka.satoru@nitech.ac.jp (S. Onaka).

0022-328X/$ - see front matter © 2004 Elsevier B.V. All rights reserved.
doi:10.1016/j.jorganchem.2004.10.061

coordinating ability of resulting Au–S derivatives to other transition metal(s) through a pyridine N atom. This paper describes the synthesis and X-ray structure analysis of new Au(I) supramolecules, $[(1,3\text{-}S_2\text{–}C_6H_4)\text{-}\{AuP(C_6H_4\text{–}3\text{-}CF_3)_3\}_2]_n$ (**1**), $[(1,4\text{-}S_2\text{–}C_6H_4)\{AuP(C_6H_4\text{–}3\text{-}CF_3)_3\}_2]_n$ (**2**), $(1,4\text{-}S_2\text{–}C_6H_4)\{AuP(C_6H_5)_2(2\text{-pyridine})\}_2$ (**3**), $[(1,3,5\text{-}S_3\text{–}C_6H_3)\{AuP(C_6H_5)_2(2\text{-pyridine})\}_3]_n$ (**4**), and $[(1,3,5\text{-}S_3\text{–}C_6H_3)\{AuP(C_6H_4\text{–}3\text{-}CF_3)_3\}_3]_n$ (**5**). Infinite polymers have been obtained for **1**, **2**, **4**, and **5**.

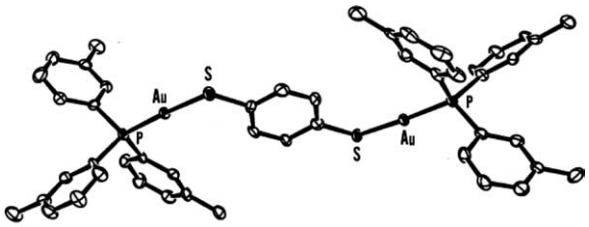

Fig. 2. An ORTEP drawing of $(1,4\text{-}S_2\text{–}C_6H_4)\{AuP(C_6H_4\text{–}3\text{-}CF_3)_3\}_2$ (**2**). F atoms are omitted for clarity.

2. Results and discussion

2.1. X-ray molecular structural analysis

The pyridyl N atoms for **3** and **4** have been determined mainly by respective Fourier peak heights. An additional reasoning for the determination of N atom is based on the absence of an aromatic hydrogen peak in the Fourier map around the assumed atom.

Fig. 1 shows an ORTEP drawing of the molecular structure of **1**. An interesting structural feature of **1** is that the two P–Au–S moieties are bent to come close intramolecularly in spite of the sterical crowding due to bulky PR'_3 groups. A plausible explanation is that two phenyl groups (C21–C26 and C51–C56), each of which comes from different PR'_3 ligands, are bent to form a preferable intramolecular π–π interaction; the detail of this stack is discussed below. When 1,4-dithiol was used as a scaffold, **2** was obtained in a good yield and two P–Au–S moieties are bent to the same rotational direction in contrast to **1** (Fig. 2). When this dithiol and PPh_2(2-pyridine) were used, **3** was obtained in a good yield; two P–Au–S moieties are bent to the same rotational direction as in **2** (Fig. 3). The $1,3,5\text{-}S_3C_6H_3$ scaffold affords **4** and **5**. The molecular structure of **4** is shown in Fig. 4. Three P–Au–S groups are bent to the same rotational direction as in **2** and **3**, thus forming a propeller-like structure. Fig. 5 shows the molecular structure of **5**, which is similar to that of **4** and a known trimercapto-triazine–Au–PPh_3 analogue [10]. No intramolecular Au–Au interaction is observed for all of these derivatives when two independently refined moieties are treated as a molecule for **2**. However, intermolecular

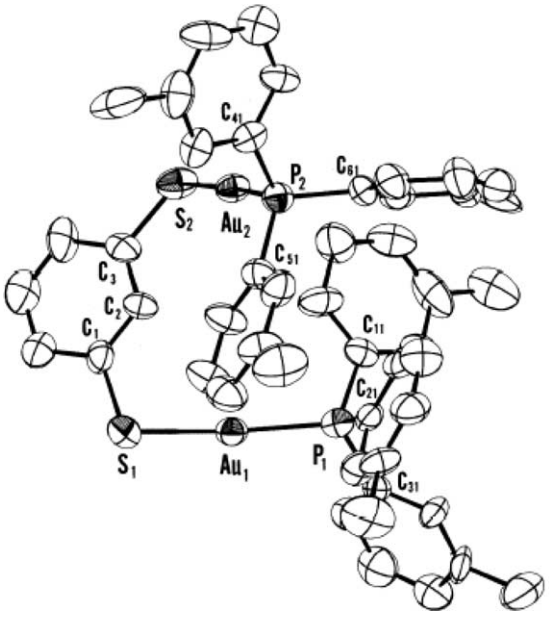

Fig. 1. An ORTEP drawing of $(1,3\text{-}S_2\text{–}C_6H_4)\{AuP(C_6H_4\text{–}3\text{-}CF_3)_3\}_2$ (**1**). F atoms are omitted for clarity.

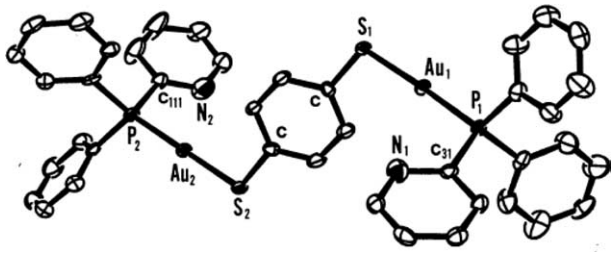

Fig. 3. The molecular structure of $(1,4\text{-}S_2\text{–}C_6H_4)\{AuP(C_6H_5)_2(2\text{-pyridine})\}_2$ (**3**).

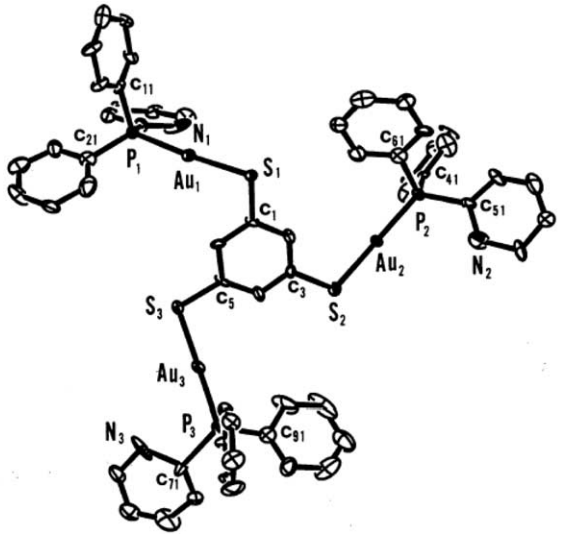

Fig. 4. The molecular structure of $(1,3,5\text{-}S_3\text{–}C_6H_3)\{AuP(C_6H_5)_2(2\text{-pyridine})\}_3$ (**4**).

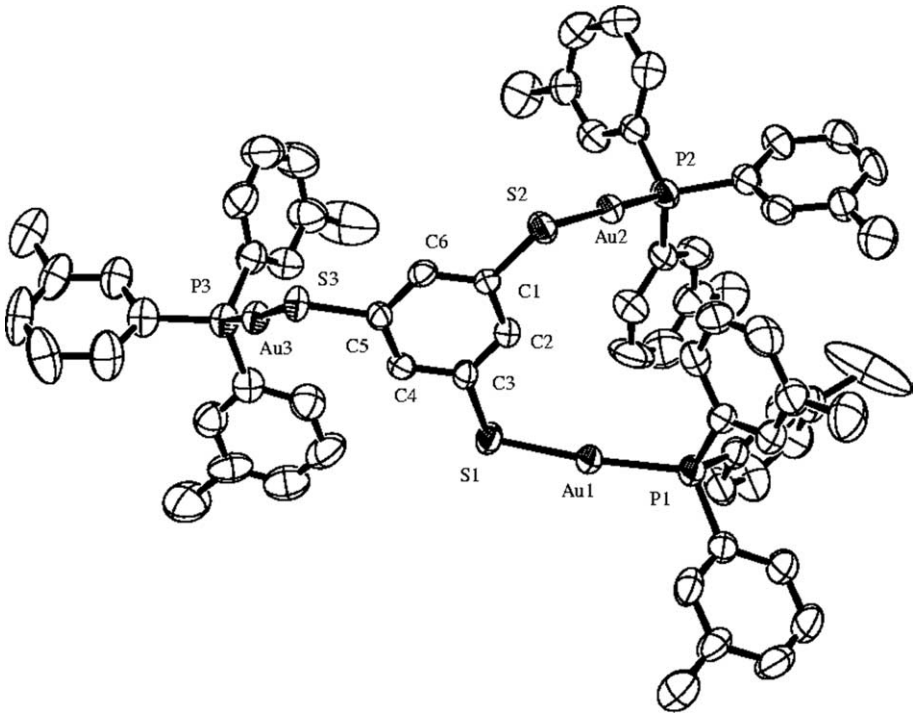

Fig. 5. An ORTEP drawing of (1,3,5-S_3–C_6H_3){AuP(C_6H_4–3-CF_3)$_3$}$_3$ (**5**). F atoms are omitted for clarity.

aurophilic interaction has been induced for **1**, **2**, **4**, and **5**. The Au–Au distance is 3.001 (1) Å for **1** and 2.992 Å (Au1–Au3) and 2.971 Å (Au2–Au4) for **2**, while the distance is 3.059 (1) Å for **4** and 3.0909(5) Å for **5**, respectively. The Au–Au distance in **1** is significantly shorter than that of the PPh_3 analogue (3.0834(8) Å) [7a] and the Au–Au distances in **2** are shorter than that of **1**. The previous paper demonstrated that the introduction of a bulky CF_3 substituent at a *meta*-position of each phenyl group in P(C_6H_5)$_3$ induces aurophilicity even for simple AuClPR_3-type compounds [4b]. Perhaps the same mechanism is effective on reinforcing the aurophilicity in **1** as in the case of our previous study. The structural details of the resulting supramolecules are described in the crystal packing section. The Au–S bond lengths are about 2.31 Å for the present series of compounds and the Au–P distances are about 2.26 Å, both of which are close to those of known PPh_3–thiolate Au(I) derivatives [4]. P–Au–S bond angles for these new compounds are almost linear (Table 2). Au–Au–S angles are acute (about 80°), while Au–Au–P angles are obtuse (about 105°) for **1**, **4**, and **5** where aurophilic interactions are operative. However, these angles come close to 90° in **2**. A glance of the molecular structure of **4** suggested that the $Au_3S_3P_3C_6$ core forms a plane. However, the deviation from the best plane defined by the $Au_3S_3P_3C_6$ core is significant for P1 (1.162 Å) and S1 (1.289 Å), which are bonded to Au1. Au1 is involved in the intermolecular Au–Au interaction. The aurophilic interaction should induce such a molecular deformation. In **5**, where the sterically more demanding phosphine ligand is used, only S_3C_6 group of the $Au_3P_3S_3C_6$ core forms a plane and the deviations from the best plane are especially large for P atoms. Otherwise, the Au–S and Au–P lengths for **5** are quite close to those of **4**.

It is interesting to compare bonding parameters of **1**–**5** with those of similar Au(I)-PPh_3 derivatives constructed on 1,3-S_2–C_6H_4 and trimercapto-triazine scaffolds [7a,10]. Although the Au–S and the Au–P lengths for **1** are slightly longer than those of the PPh_3 analogues, [7a] these bond lengths in **2**–**5** are little influenced by replacing the phosphine ligand from PPh_3 to PPh_2(2-py) and P(C_6H_4–3-CF_3)$_3$ for the present series of compounds.

2.2. Crystal structures

Fig. 6 shows the crystal packing of **1** viewed along the *c*-axis, which clearly exhibits a cage structure made from Au–Au interactions (r(Au–Au) = 3.0021(7) Å) and π–π stacks. The shortest C–C distance among the carbon atoms of the 1,3-S_2–benzene ring (C1–C6) and those of the benzene ring (C31–C36) in AuP(C_6H_4–3-CF_3)$_3$ is 3.436 Å for C4 and C33. In addition, distances among C2–C6 and C31–C36 are below 4.0 Å and these two planes are almost parallel. These findings support π–π interaction between these benzene rings. It might be anticipated from a glance of Fig. 6 that π–π stacks are also operative between two C31–C36 planes. However, distances among relevant carbon atoms are beyond the range of the normal π–π interaction. In this vein, the cage formation is incomplete. However, Fig. 7 indicates

Table 1
Crystal data

Compound	**1**	**2**	**3**	**4**	**5**
Empirical formula	$C_{54}H_{28}Au_2F_{18}P_2S_2$	$C_{55}H_{36}Au_2Cl_2F_{18}P_2S_2$	$C_{40}H_{32}Au_2N_2P_2S_2$	$C_{59}H_{49}Au_3Cl_4N_3P_3S_3$	$C_{75}H_{45}Au_3F_{27}P_3S_3$
Formula weight	1516.6	3018.3	1145.6	1721.8.0	2238.1
Crystal system	Monoclinic	Monoclinic	Monoclinic	Monoclinic	Monoclinic
Space group	$P2_1/n$	Pc	$P2_1/c$	$P2_1$	$P2_1/n$
a (Å)	24.84(1)	17.426(3)	18.710(1)	8.858(2)	16.708(3)
b (Å)	16.268(9)	16.001(3)	14.6611(8)	13.744(3)	16.450(3)
c (Å)	13.728(8)	18.393(3)	15.5821(9)	23.371(5)	29.009(5)
β (°)	97.40(4)	99.580(1)	113.287(1)	91.763(4)	102.211(3)
Z	4	2	4	2	4
d_{calcd} (g cm^{-3})	1.82	1.95	1.94	2.01	1.90
Crystal dimensions (mm^3)	$0.7 \times 0.4 \times 0.3$	$0.35 \times 0.15 \times 0.15$	$0.31 \times 0.19 \times 0.07$	$0.20 \times 0.10 \times 0.10$	$0.25 \times 0.15 \times 0.1$
V (Å^3)	5501(5)	5057(2)	3926.0(4)	2844(1)	7792.6(6)
μ(Mo Kα) (cm^{-1})	55.5	60.9	78.2	81.4	58.8
Diffractometer	MAC MXC3	SMART APEX	SMART APEX	SMART APEX	SMART APEX
$2\theta_{max}$ (°)	45.0	55.0	55.0	55.0	55.0
Temperature (K)	298	100	100	100	293
Unique reflections	7179	15,890	8999	10,648	11,217
Reflections with $\|F_o\| > 3\sigma(\|F_o\|)$	5110	13,172	7937	10,320	8408
No. of parameters refined	668	1324	461	676	1066
R	0.06	0.039	0.06	0.05	0.036
Rw_2	0.17	0.054	0.17	0.12	0.083

Mo Kα radiation ($\lambda = 0.71073$ Å); $R = \sum\|\|F_o| - |F_c|\|/|F_o|$; $R_w = \{\sum(|F_o| - |F_c|)^2/\sum w(F_o)^2|^{1/2}$, where $w = 1/\sigma^2(F_o^2)$.

that each cage contains two benzene molecules with side to side and the C_6 axes of trapped benzene molecules are almost perpendicular to the cage or the channel. This finding supports the view that the void behaves like a nano-tube; the shortest edge-to-edge distance (S–S) is 10.0 Å, while the longest distance (P–P) is 17.3 Å. Thus, formed nano-channels are fused together to yield a distorted honeycomb structure. Quite interestingly, the PPh_3 analogue of **1** does not provide such a channel-like structure according to Laguna and co-workers [7a]. The thermogravimetric analysis has shown that **1** loses its weight slowly above 120 °C, sharply above 139 °C, and color changes from pale yellow to yellow. The resulting solid is not soluble in common laboratory solvents, which suggests that the channel structure is destroyed upon the loss of benzene molecules.

The $(1,4\text{-}S_2\text{–}C_6H_4)\{AuP(C_6H_4\text{–}3\text{-}CF_3)_3\}_2$ unit is self-assembled by aurophilicity at two opposite sites of the $1,4\text{-}S_2\text{–}C_6H_4$ scaffold to afford an 8 (eight)-shaped helix (Fig. 8(a) and (b)) for **2**; the main helical axis is parallel to the c-axis. Aurophilicity plays a crucial role in constructing the helix like a hydrogen bond for protein helices and/or DNA. The details of the helical structure are described below. ^{31}P NMR shows a singlet at the highest field among these five derivatives (δ 31.9). The helical structure should be responsible for this high-field shift.

The crystal-packing diagrams for **4** and **5** demonstrate the formation of quasi one-dimensional chains composed mainly of aurophilic interaction, the skeletons of which look like the teeth of a saw (Figs. 9 and 10). Fig. 9 also demonstrates that three P–Au–S moieties in a unit are almost parallel to the corresponding three P–Au–S moieties of neighboring molecules. Detailed inspection of the crystal-packing does not indicate significant π–π stacks among aromatic rings, including pyridine in **4**. Each void of crystals for **2** and **4** contains solvent CH_2Cl_2 molecule.

It is amazing that the solid structures of **2** and **3** are dramatically changed by only slightly modifying the aryl phosphine ligand as was described above. Neither infinite chain nor helix is formed for **3**. Although the substituent effect of the CF_3 group at a *meta*-position on the aurophilicity was demonstrated in the previous paper, [4b] it was supposed from recent developments in crystal engineering [14,15] that the hydrogen bond may assist the formation of the helix in **2**. Therefore, a source of hydrogen bond was sought among F atoms and aromatic hydrogens in the molecular packing diagram in **2**. Two hydrogen atoms (H2 and H5) in the core $1,4\text{-}S_2\text{–}C_6H_4$ pedestal are involved in hydrogen bonds with one of the F atoms in a CF_3 substituent of the $(3\text{-}CF_3\text{–}C_6H_4)_3P$ ligand; r(H–F) = 2.608 and 2.649 Å. Fig. 11 shows a part of the hydrogen bonds among these atoms. These hydrogen bonds may assist the formation of an 8-shaped loop. However, it is apparent that the aurophilicity plays the crucial role for the present "double helix" formation. This work affords another example of the essential contribution of aurophilicity to construct an "artificial DNA" other than hydrogen bonds. Recently, Puddephatt et al. [16] have reported quite interesting helical loops in self-assembled polymers in which aurophilicity plays a crucial role. Lippert et al. [17] have also reported interesting molecular architectures composed of Ag ions and 2,2′-bipyrazine and classified them into an infinite helix, an infinite chain, and an infinite loop. Our

Table 2
Selected bond lengths (Å) and angles (°)

Compounds	**1**	**2**	**3**	**4**	**5**
Au–Au	3.001(1)	2.9714(8)		3.055(7)	3.0909(5)
		2.9923(8)			
Au–S	2.330(5)	2.339(3)	2.309(2)	2.318(3)	2.308(2)
	2.320(4)		2.306(2)	2.325(6)	2.312(2)
		2.315(3)		2.293(3)	2.297 (2)
		2.303(3)			
Au–P	2.271(5)	2.227(3)	2.262(2)	2.269(3)	2.259(2)
	2.274(4)	2.297(3)	2.264(2)	2.268(3)	2.265(2)
		2.260(3)		2.266(3)	2.246(3)
		2.270(3)			
S–C	1.76(2)	1.77(1)	1.772(8)	1.77(2)	1.769(8)
	1.76(2)	1.77(1)	1.774(8)	1.79(3)	1.781(7)
		1.76(1)		1.77(2)	1.781(7)
		1.79(1)			
P–C	1.81(2)	1.81(1)	1.819(7)	1.85(2)	1.826(9)
	1.83(2)	1.82(1)	1.830(8)	1.84(2)	1.821(9)
	1.83(2)	1.83(1)	1.818(7)	1.83(2)	1.817(8)
		1.80(1)	1.823(7)	1.84(2)	1.814(8)
		1.83(1)	1.822(8)	1.81(2)	1.814(9)
		1.82(1)	1.825(7)	1.86(2)	1.814(9)
					1.814(8)
		1.82(1)			1.81(1)
		1.82(1)			1.81(1)
		1.80(1)			
		1.83(1)			
		1.82(1)			
		1.82(1)			
P–Au–S	172.6(2)	176.3(1)	176.30(6)	172.5(2)	173.33(4)
	174.1(2)		177.90(6)	172.7(2)	174.52(7)
		174.0(1)		178.8(2)	173.11(9)
		176.6(1)			
Au–S–C	101.1(6)	106.5(4)	105.8(3)	103.5(7)	101.7(3)
	105.0(6)		107.4(3)	108.6(7)	103.6(3)
		106.2(4)		105.7(7)	105.0(3)
		107.4(4)			
Au–P–C	114.0(10)	113.8(4)	114.1(2)	110.7(7)	113.3(3)
	105.3(6)	115.6(4)	112.7(3)	113.6(7)	110.5(3)
	116.8(5)	113.8(4)	112.2(2)	112.6(6)	119.2(3)
	111.8(5)	112.4(4)	111.4(2)	119.1(7)	115.7(3)
	111.0(6)	112.1(4)	113.4(2)	112.8(8)	114.9(3)
	118.1(6)	115.3(4)	115.8(2)	108.1(8)	108.9(3)
		112.0(4)		118.2(9)	113.8(3)
		111.7(4)		113.2(7)	111.1(3)
		114.7(4)		112.3(9)	114.0(3)
		112.3(4)			
		115.1(4)			
		112.7(3)			
Au–Au–S	81.4(1)	85.77(7)		76.4(1)	85.68(5)
	81.3(1)	83.08(8)		76.2(1)	81.06(5)
		80.48(8)			
Au–Au–P	105.4(1)	97.21(8)		106.7(1)	89.38(6)
	100.7(1)	101.34(8)		111.1(1)	97.28(6)
		102.92(8)			

"double helix" in **2** belongs to an infinite loop. Finally, we would like to point out the possible contribution of the present type of manifestation of aurophilicity to the gold-sensing of DNA which has been highlighted recently [13].

Synthesis of gold dendrimers has recently been targeted for preparing gold nano-particles, [3] establishing drug-delivery systems, and/or generating new intelligent nano-materials [18]. Symmetric S_3 pedestals are quite promising to construct dendrimers by the use of

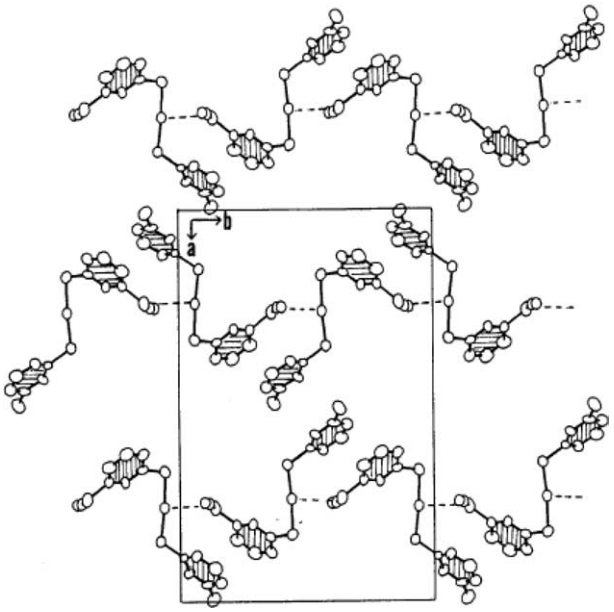

Fig. 6. A crystal packing diagram of **1** along the *c*-axis. Only important molecular parts are shown for clarity. The dotted · line (· · ·) indicates Au–Au interaction and hatched rings are concerned with π–π interactions.

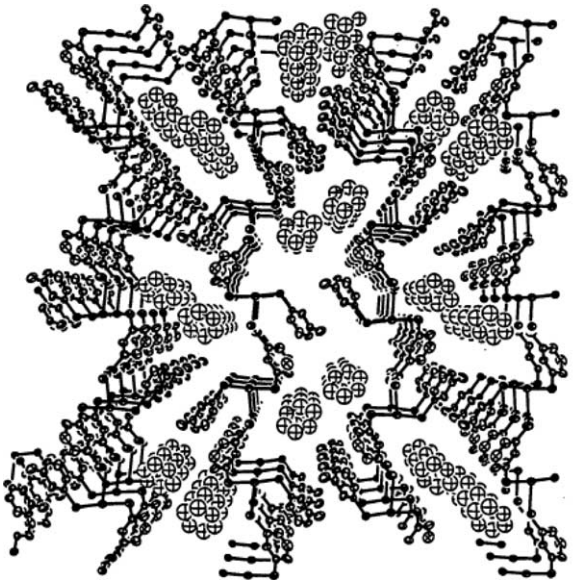

Fig. 7. Benzene-filled channels in **1**. Channels are almost along the *c*-axis direction.

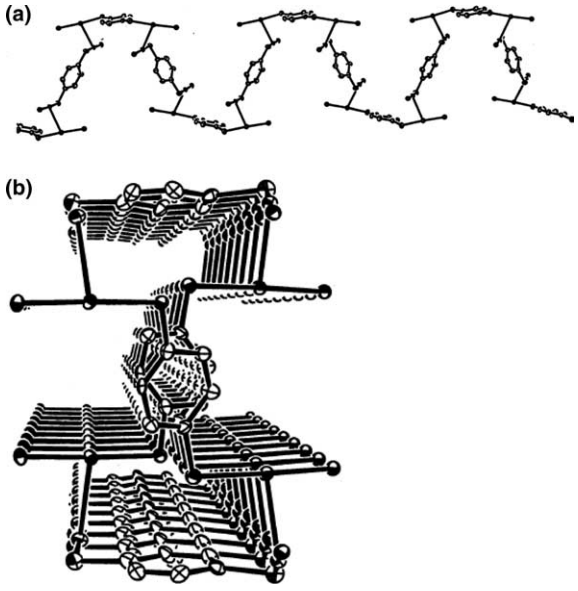

Fig. 8. (a) A crystal packing diagram of **2** which exhibits an infinite chain structure (side view). (b) A crystal packing diagram of **2** which exhibits an 8-shaped "double helix" (top view).

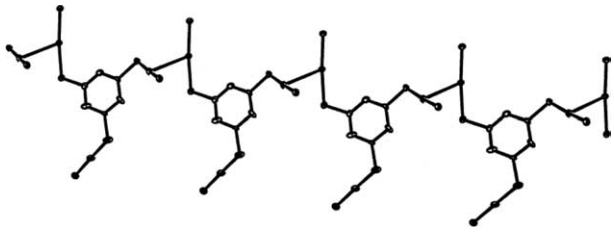

Fig. 9. A crystal packing diagram of **4** which exhibits an infinite quasi one-dimensional chain, the skeleton of which is similar to saw-toothed.

divergent procedures. In this vein, **4** and **5** are quite interesting as a kind of "dendrimer". Several attempts have been made to generate a higher "dendrimer" by connecting the pyridine-N in each PPh_2(2-py) ligand for **3** and **4** with other Au(I) and/or heterometal components. Successful outcomes have not been obtained because N-positions in this ligand are not suitable for constructing such oligomers. Therefore, another selection of PPh_2(py) ligands in which N is located at a 3- or 4-position has been attempted and efforts for constructing a "larger dendrimer" are continuing in this laboratory. Our recent paper has proved that this kind of strategy is quite promising for constructing heteronuclear supramolecules by the use of Au(S–4py)PR_3 as a building block [19].

3. Experimental

3.1. General comments

Reactions were carried out under an argon atmosphere by standard Schlenk techniques. The reaction vessel was covered with a piece of black cloth. The PPh_2(2-pyridyl) ligand was purchased from Aldrich. $P(C_6H_4$–3-$CF_3)_3$ was synthesized as reported previously [4b]. 1,3-Benzenedithiol, 1,4-benzenedithiol, and 1,3,5-benzenetrithiol were purchased from Nihon Fine-chemicals Co. Ltd.

$^{31}P\{^1H\}$ NMR spectra were recorded on a Varian XL-200 spectrometer at 80.984 MHz. $^{31}P\{^1H\}$ NMR

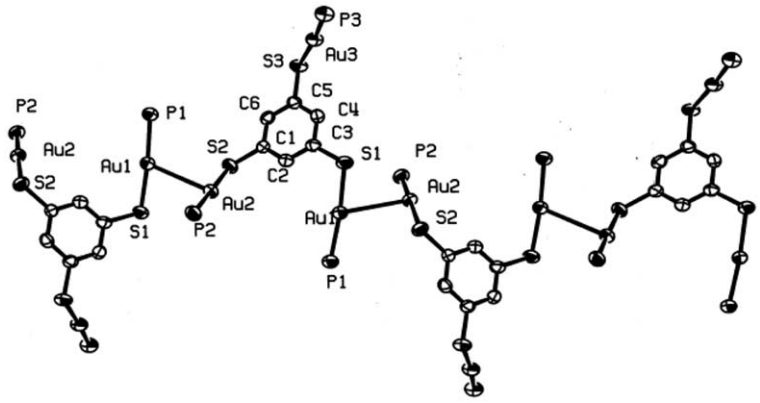

Fig. 10. A crystal packing diagram of **5** which exhibits an infinite quasi one-dimensional chain.

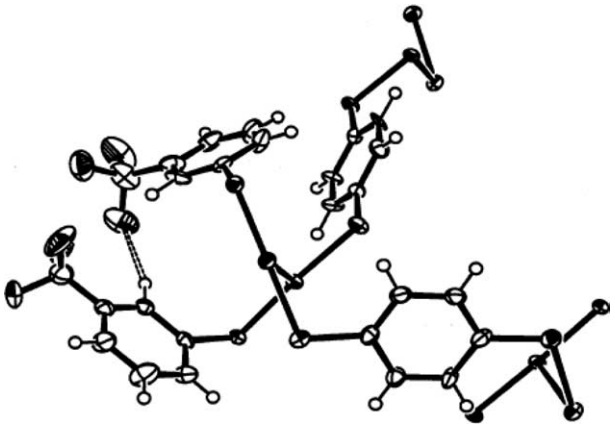

Fig. 11. One of the hydrogen bonds between an F atom of the CF_3 and an aromatic hydrogen for **2**.

chemical shifts are referenced to external 85% H_3PO_4.

3.2. *(1,3-S_2–C_6H_4){AuP(C_6H_4–3-CF_3)$_3$}$_2$ (**1**)*

700 mg (1 mmol) of AuClP(C_6H_4–3-CF_3)$_3$ was dissolved in mixed solvents of CH_2Cl_2 (20 ml) and acetone (30 ml). To this was added methanol solution (40 ml) of 1,3-benzenedithiol (71 mg, 0.5 mmol) and KOH (68 mg), and the mixture was stirred at room temperature overnight. Solvents were distilled off at reduced pressure and the resulting pale yellow solid was washed with small amounts of methanol, hexane, and benzene successively. The residue was extracted with each 10 ml of CH_2Cl_2 two times and the solvent was partially distilled at reduced pressure. Then, small amount of benzene was added and the mixture was stored in a refrigerator to afford pale yellow crystals of **1**. Yield 520 mg in the form of single crystals, 71%. Low solubility of this molecule in ordinary organic solvents made it impossible to obtain a ^{31}P NMR spectrum. Anal. Calc. for $C_{48}H_{28}Au_2F_{18}P_2S_2 \cdot C_6H_6$: C, 41.98; H, 2.22%. Found: C, 42.11; H, 2.50%.

3.3. *(1,4-S_2–C_6H_4){AuP(C_6H_4–3-CF_3)$_3$}$_2 \cdot C_6H_6 \cdot CH_2Cl_2$ (**2**)*

160 mg (0.23 mmol) of AuClP(3-CF_3–C_6H_4)$_3$ was dissolved in 2 ml of CH_2Cl_2. To this was added dichloromethane solution (1 ml) of 1,4-benzenedithiol (17 mg, 0.12 mmol) and the mixture was stirred at room temperature overnight. Solvents were distilled off at reduced pressure and the resulting yellow solid was recrystallized from CH_2Cl_2/benzene to afford bright yellow crystals of **2**. Yield 120 mg, 72%. $^{31}P\{^1H\}$ NMR ($CDCl_3$); δ 31.9. Anal. Calc. for $C_{48}H_{28}Au_2F_{18}P_2S_2 \cdot CH_2Cl_2 \cdot C_6H_6$: C, 40.53; H, 2.22%. Found: C, 40.91 ; H, 2.06%.

3.4. *(1,4-S_2–C_6H_4){AuP(C_6H_5)$_2$(2-pyridine)}$_2$ (**3**)*

200 mg (0.4 mmol) of AuClP(C_6H_4)$_2$(2-pyridine) was dissolved in 30 ml of CH_2Cl_2. To this was added methanol solution (12 ml) of 1,4-benzenedithiol (28 mg, 0.2 mmol) and Na_2CO_3 (430 mg, 4 mmol), and the mixture was stirred at room temperature for 2 h. Solvents were distilled off at reduced pressure and the resulting pale yellow solid was extracted with each 5 ml of CH_2Cl_2 two times. Then, the solvent was distilled at reduced pressure. The residue was recrystallized from CH_2Cl_2/hexane to afford pale yellow crystals of **3**. Yield 155 mg, 73%. $^{31}P\{^1H\}$ NMR ($CDCl_3$); δ 38.1. Anal. Calc. for $C_{40}H_{32}Au_2N_2P_2S_2$ (vacuum-dried sample): C, 45.29; H, 3.04; N 2.64%. Found: C, 45.29; H, 3.09; N 2.67%.

3.5. *(1,4-S_3–C_6H_3){AuP(C_6H_5)$_2$(2-pyridine)}$_3 \cdot 2CH_2Cl_2$ (**4**)*

300 mg (0.6 mmol) of AuClP(C_6H_5)$_2$(2-pyridine) was dissolved in 30 ml of CH_2Cl_2. To this was added a methanol solution (20 ml) of 1,3,5-benzenetrithiol (35 mg, 0.2 mmol) and Na_2CO_3 (430 mg, 4 mmol), and the mixture was stirred at room temperature for 2 h. Solvents were distilled off at reduced pressure and the resulting pale

yellow solid was extracted with each 5 ml of CH_2Cl_2 two times. Then, the solvent was distilled at reduced pressure. The residue was recrystallized from CH_2Cl_2/hexane to afford pale yellow crystals of **4**. Yield 240 mg, 77%. $^{31}P\{^1H\}$ NMR ($CDCl_3$); δ 38.3. Anal. Calc. for $C_{57}H_{45}Au_3N_3P_3S_3 \cdot 2CH_2Cl_2$: C, 41.15; H, 2.87; N, 2.44%. Found: C, 41.39 ; H, 2.93; N, 2.38%.

3.6. (1,3,5-S_3–C_6H_3){AuP(C_6H_4–3-CF_3)$_3$}$_3$ · C_6H_6 (5)

210 mg (0.3 mmol) of AuClP(C_6H_4–3-CF_3)$_3$ was dissolved in 15 ml of CH_2Cl_2. This solution was dropped into a methanol solution (5 ml) of 1,3,5-benzenetrithiol (18 mg, 0.1 mmol) and KOH (17 mg), and the mixture was stirred at room temperature for 1 h. The solution was subjected to filtration and the solvent was distilled off at reduced pressure. The resulting solid was extracted with benzene–CH_2Cl_2 to give yellow solids **5**. Yield 160 mg, 75%. Single crystals were grown from CH_2Cl_2/hexane. $^{31}P\{^1H\}$ NMR ($CDCl_3$); δ 35.3. Anal. Calc. for $C_{75}H_{45}Au_3F_{27}P_3S_3$; C, 40.23; H, 2.03%. Found: C, 39.94 ; H, 1.87%.

3.7. X-ray crystallography

Selected crystals of **1** and **5** were glued to the top of a fine glass rod for room temperature measurements and selected crystals of other compounds **2**–**4** were attached on a nylon loop for 100 K measurements. The reflection data for **1** were collected by use of a MAC MXC3 diffractometer with graphite-monochromated Mo Kα radiation (λ = 0.71073 Å) and those for **2**–**5** were collected on a Bruker SMART-APEX CCD diffractometer with graphite-monochromated Mo Kα radiation (λ = 0.71073 Å) at 100 K. The structures of these crystals were solved by direct method using Sir-97 in a WinGx program package and refined with anisotropic thermal parameters by full-matrix least-squares programs on SHELXS-97 in a WinGx program package [20]. The refinements were made on F^2 data and the final R and wR_2 values are given in Table 2. Tables for atomic coordinates, thermal parameters, and bond lengths and angles are available as supplementary materials. Selected bond lengths and angles are given in Table 1. The supplementary crystallographic data are contained in CCDC 227471 (**1**), 227473 (**2**), 227472 (**3**), 227469 (**4**), and 237195 (**5**).

Acknowledgments

This research was funded by Grants-in Aid for Scientific research on Priority Area (No. 11136218, No. 12023221 ''Metal-assembled Complexes'') and by Grants-in Aid for Scientific research (No. 14540514 (S.O.) and 15550047 (T.O.)) from the Ministry of Education, Science, Sports and Culture, Japan. Thanks are also due to CREST, JST (T.O.).

References

[1] B.J. Holliday, C.A. Mirkin, Angew. Chem. Int. Ed. 40 (2001) 2022, and references therein.
[2] A. Müller, H. Reuter, S. Dillinger, Angew. Chem. Int. Ed. 34 (1995) 2328;
R.W. Saalfrank, B. Demleitner, in: J.-P. Sauvage (Ed.), Transition Metals in Supramolecular Chemistry, Perspectives in Supramolecular Chemistry, vol. 5, Wiley–VCH, Weinheim, 1999, p. 1, and references therein.
[3] D. Shmid (Ed.), Clusters and Colloids, VCH, Weinheim, 1994;
H. Schmidbaur (Ed.), Gold, Wiley, Chichester, 1999;
C. Joachim, S. Roth (Eds.), Atomic and Molecular Wires, Kluwer, Dordrecht, 1997;
G.D. Mendenhall, A. Greenberg, J.F. Liebma, Molecules – from Molecules to Materials, Chapman & Hall, London, 1995, and references therein.
[4] (a) T. Yoshida, S. Onaka, M. Shiotsuka, Inorg. Chim. Acta 342 (2003) 319;
(b) K. Nunokawa, S. Onaka, T. Tatematsu, M. Ito, J. Sakai, Inorg. Chim. Acta 322 (2001) 56;
(c) S. Onaka, Y. Katsukawa, M. Shiotsuka, O. Kanegawa, M. Yamashita, Inorg. Chim. Acta 312 (2001) 100;
(d) K. Nunokawa, T. Sunahara, S. Onaka, K. Okazaki, H. Imai, K. Inoue, T. Ozeki, Chem. Lett. 33 (10) (2004) 1300.
[5] M. Nakamoto, H. Koijman, M. Paul, W. Hiller, H. Schmidbaur, Z. anorg. Allg. Chem. 619 (1993) 1341.
[6] R.M. Dàvila, A. Elduque, T. Grant, R.J. Staples, J.P. Facjler Jr., Inorg. Chem. 32 (1993) 1749.
[7] (a) M.C. Gimeno, P.G. jones, A. Laguna, M. Laguna, R. Terroba, Inorg. Chem. 33 (1994) 3932;
(b) I. del Rio, R. Terroba, E. Cerrada, M.B. Hursthouse, M. Laguna, M.E. Light, A. Ruiz, Eur. J. Inorg. Chem. (2001) 2013, and references therein.
[8] B.-C. Tzeng, C.-M. Che, S.-M. Peng, J. Chem. Soc. Chem. Commun. (1997) 1771.
[9] K. Henke, D.A. Atwood, Inorg. Chem. 37 (1998) 224;
K. Henke, A.R. Hutchinson, M.K. Krepps, S. Parkin, D.A. Atwood, Inorg. Chem. 40 (2001) 4443.
[10] W.J. Hunks, M.C. Jennings, R.J. Puddephatt, Inorg. Chem. 38 (1999) 5930.
[11] M. Hong, Y. Zhao, W. Su, R. Cao, M. Fujita, Z. Zhou, A.S.C. Chan, Angew. Chem. Int. Ed. 39 (2000) 2468.
[12] J.D.E.T. Wilton-Ely, A. Schier, N.W. Mitzel, H. Schmidbaur, Inorg. Chem. 40 (2001) 6266.
[13] C.A. Mirkin, R.L. Letsinger, R.C. Mucic, J.J. Storhoff, Nature 382 (1996) 607;
R. Elghanian, J.C. Storhoff, R.C. Mucic, R.L. Letsinger, C.A. Mirkin, Science 277 (1997) 1078.
[14] G.A. Jeffrey, An Introduction to Hydrogen Bonding, Oxford University Press, Oxford, 1997, and references therein.
[15] G.R. Desiraju, T. Steiner, The Weak Hydrogen Bond, Oxford Science, Oxford, 1999, and references therein.
[16] R.J. Puddephatt, J. Chem. Soc. Chem. Commun. (1998) 1055;
R.J. Puddephatt, Coord. Chem. Rev. 216–217 (2001) 313;
Z. Qin, M.C. Jennings, R.J. Puddephatt, Chem. Eur. J. 8 (2002) 735.
[17] R.-D. Schnebeck, E. Freisinger, B. Lippert, Eur. J. Inorg. Chem. (2000) 1193.
[18] P. Lange, A. Schier, H. Schmidbaur, Inorg. Chem. 35 (1996) 637.
[19] K. Nunokawa, S. Onaka, Y. Mizuno, K. Okazaki, T. Sunahara, M. Ito, M. Yaguchi, H. Imai, K. Inoue, T. Ozeki, H. Chiba, T. Yoshida, J. Organomet. Chem. 690 (2004) 48.
[20] G.M. Sheldrick, SHELX-97, Program for Analysis of Crystal Structures, University of Götiingen, Germany, 1997.